Protein arginine methyltransferases as modulators of lipid metabolism and inflammation and the relevance for atherosclerosis

Zhang, Y.

Chapter

PRMT1

Chapter 2

PRMT1 inhibitor TC-E 5003 reduces the development of non-alcoholic fatty liver disease and atherosclerotic lesions in Western-type diet-fed LDL receptor knockout mice

Yiheng Zhang^*, Timothy J.P. Sijsenaar*, Mireia N.A. Bernabé Klein, Ezra J. van der Wel, Miranda Van Eck, Menno Hoekstra

Division of BioTherapeutics, Leiden Academic Centre for Drug Research (LACDR), Leiden University, Gorlaeus Laboratories, Einsteinweg 55, 2333CC Leiden, The Netherlands

* Authors contributed equally

^ Corresponding author:

ABSTRACT

Background/Aim: Non-alcoholic fatty liver disease (NAFLD), characterized by increased hepatic lipogenesis and triglyceride accumulation, predisposes to atherosclerotic cardiovascular disease. In vitro studies have suggested that protein arginine methyltransferase 1 (PRMT1) is a functional transcriptional co-activator of the lipogenic program in hepatocytes. Here we evaluated the potential of PRMT1 inhibitor TC-E 5003 to lower NAFLD and atherosclerosis susceptibility in vivo.

Methods: Male low-density lipoprotein receptor knockout mice were fed a Western-type diet and injected intraperitoneally 3x/week with 10 mg/kg TC-E 5003 or solvent control for 8 weeks.

Results: TC-E 5003 treatment was associated with a 42% decrease ($P<0.01$) in hepatic mRNA expression levels of fatty acid synthase. In accordance, liver triglyceride stores were 33% ($P<0.05$) lower upon PRMT1 inhibition, without a change in tissue cholesterol levels. Concomitant 33% to 40% reductions ($P<0.05$) in plasma cholesterol and triglyceride levels, respectively, were detected in TC-E 5003-treated mice, which could be attributed to a decrease in very-low-density and low-density lipoprotein levels. PRMT1 inhibition was associated with a trend towards a reduction in aortic root Oil red O+ area (-25%; $P=0.11$) and a significant decrease in CD68+ macrophage content (-57%; $P<0.05$). This coincided with shifts in splenic monocyte and T cell polarization towards the anti-inflammatory $Ly6C^{low}$ and pro-inflammatory effector memory phenotypes, respectively.

Conclusions: We have shown that PRMT1 inhibition is associated with reduced hepatic triglyceride accumulation, hyperlipidemia and splenic monocyte activation in the context of increased T cell activation, resulting in an overall decrease in atherosclerosis susceptibility in Western-type diet-fed LDL receptor knockout mice.

KEYWORDS: protein arginine methyltransferase 1; lipoprotein; lipid metabolism; atherosclerosis; inflammation; fatty liver disease

INTRODUCTION

Cardiovascular disease and its underlying pathology, atherosclerosis, are regarded as the most common causes of death worldwide[1,2]. Higher levels of lipids in plasma, i.e. high very-low-density lipoprotein (VLDL)-triglyceride and low-density lipoprotein (LDL)-cholesterol levels, are strongly associated with an increased risk for developing atherosclerosis [3]. Since the liver plays an important role in the maintenance of plasma lipid homeostasis, dysfunction of liver lipid metabolism can affect plasma lipid levels. People with non-alcoholic fatty liver disease (NAFLD, characterized by triglyceride accumulation in hepatocytes, display an increased chance of developing hyperlipidemia and a higher risk of atherosclerosis [4,5]. Mechanistically, NAFLD patients exhibit an over-activated hepatic de novo lipogenesis, subsequently leading to a hyperactive production and secretion of pro-atherogenic VLDL particles by the liver. Therefore, we hypothesize that targeting hepatic lipogenesis in NAFLD is a therapeutic strategy to prevent the consequent hyperlipidemia and atherosclerosis susceptibility.

The study by Park et al. suggested that protein arginine methyl transferase 1(PRMT1)is a potential therapeutic target for the treatment of NAFLD and its correlated diseases. More specifically, their human study indicated that PRMT1 exhibits an elevated expression level in livers of NAFLD patients compared to healthy livers. In addition, both their in vitro and in vivo studies showed that PRMT1 is involved in hepatic lipogenesis as an transcriptional modulator [6]. In further support, another study by Choi et. al. found that hepatocyte-specific knockdown of PRMT1 in mice downregulates the mRNA expression levels of lipogenic genes FASN and SREBP1C. However, the functional effect of a diminished PRMT1 function on NAFLD and its co-morbidities is currently not yet known.

TC-E 5003 was discovered and verified as a specific inhibitor for PRMT1 to investigate its physiological roles in vitro and in vivo [7]. Previous studies have shown that the atherogenic diet-induced hypercholesterolemia and associated susceptibility for atherosclerosis in LDL receptor knockout mice are driven by hyperactive hepatic lipogenesis [8]. To verify our hypothesis that PRMT1 inhibition can lower triglyceride synthesis in liver and thereby correct dyslipidemia, in the current study we therefore investigated the effect of long-term TC-E 5003 treatment on hepatic and plasma lipid levels and atherosclerosis susceptibility in LDL receptor knockout mice.

MATERIALS AND METHODS

Experimental animals

Twenty-two 10-week-old male LDL receptor knockout mice, obtained from The Jackson Laboratory and bred at Gorlaeus Laboratories, were fed a Western-type diet containing 0.25% cholesterol and 15% cocoa butter (SDS, Sussex, UK) to induce the development of atherosclerotic lesions. The mice were randomly allocated to two different treatment groups receiving intraperitoneal injections of either the control solvent DMSO (Control; 10 µL (~350 mg/kg); N = 11) or TC-E 5003 (TC-E; 10 mg/kg in DMSO; N = 11; Tocris Biosciences) three times per week. Over the course of the experiment, two of the mice belonging to the TC-E group were found dead in their cage in treatment week 2 and week 5, respectively. In addition, one TC-E-treated mouse had to be sacrificed in week 6 as it had lost more than 15% of its original body weight (primary human endpoint). All data gathered from these 3 mice up to this point were eliminated from further analysis. At the 8-week mark, a fourth mouse belonging to the TC-E group started to lose weight and it was therefore decided to terminate the study early so as to maintain a large enough group size to measure treatment-specific effects. Hence, the 19 remaining mice were anesthetized through a subcutaneous injection with 100-150 µl of a ketamine (100 mg/kg), xylazine (12.5 mg/kg), and atropine (125 µg/kg) mixture. Subsequently, orbital blood was collected and a whole-body perfusion was performed using phosphate buffered saline (PBS). Organs were excised and parts were fixed for 24 hours in a 3.7% formalin solution for subsequent histological analysis or stored at -20℃ for following biochemical analysis.

All experimental protocols were approved by the Animal Welfare Body of Leiden University under the project license AVD1060020185964 issued by the Central Authority for Scientific Procedures on Animals (CCD). The study was

executed according to the principles of laboratory animal care and regulations of Dutch law on animal welfare, the Directive 2010/63/EU of the European Union, and the ARRIVE guidelines.

Blood glucose measurements

Blood glucose levels were measured after 5 weeks of treatment by tail bleeding using a Bayer Contour TS glucose meter (Leverkusen, Germany).

Plasma lipid measurements

Plasma specimens were isolated from orbital blood samples, collected at sacrifice, after 5-minute centrifugation at 6000 rpm. Plasma concentrations of free cholesterol, cholesterol esters, and triglycerides were determined using enzymatic colorimetric assays (Roche Diagnostics). The distribution of cholesterol over the different lipoproteins was analyzed through fractionation of a pooled plasma sample from the control and treatment groups using fast protein liquid chromatography by ÄKTA go (GE Healthcare) with a Superose 6 column. For each colorimetric assay, precipath (Roche Diagnostics) was used as internal calibrator.

Liver tissue lipid extraction and quantification

Triglyceride and cholesterol were extracted from ~50 mg of liver per mouse. For triglyceride extraction, the liver pieces were homogenized in 500 µl 5% Nonidet™ P 40 Substitute. The solution was heated at 90℃ and cooled on ice for 2 minutes each. Subsequently, insoluble material was removed from the solution through centrifugation and triglycerides in the supernatant were measured using an enzymatic colorimetric assay (Roche Diagnostics). Cholesterol was extracted using the protocol of Bligh and Dyer [9] and quantified using an enzymatic colorimetric assay. The concentration of triglycerides and cholesterol in liver samples was corrected for the amount of tissue protein and expressed as µg lipid / mg protein.

Gene expression analysis through real-time quantitative PCR

RNA was isolated using the standard phenol / chloroform extraction method. The concentration of the obtained RNA was determined using a Nanodrop Spectrophotometer (Nanodrop Technologies, Wilmington, DE, USA). cDNA was synthesized from the RNA using Maxima H Minus reverse transcriptase (Thermo Scientific). Analysis of gene expression was accomplished through an ABI PRSM 7500 machine (Applied Biosystems, Foster City, CA) using SYBR Green technology. The genes β-actin, ribosomal protein L27 (RPL27), acidic ribosomal phosphoprotein P0 (36B4) and peptidylpropyl isomerase A (PPIA) were used as housekeeping genes. The sequences of the primers used can be found in Table 1.

Table 1: Nucleotide sequences of primers used for RT-PCR

GENE	GENBANK ACCESSION NO.	FORWARD PRIMER	REVERSE PRIMER
PPIA	NM_008907.2	AGGATTTGGCTATAAGGGTTCCTCC	ATTTCTCTCCGTAGATGGACCTGC
RPL27	NM_011289.3	CGCCAAGCGATCCAAGATCAAGTCC	AGCTGGGTCCCTGAACACATCCTTG
36b4	NM_007475.5	CTGAGTACACCTTCCCACTTACTGA	CGACTCTTCCTTTGCTTCAGCTTT
MYH7	NM_080728.3	AATGCAGAGTCAGTGAAGGGCATG	CTTGTAGGCCTTCACCTTCAGCTG
NPPA	NM_008725.3	AAAAGCAAACTGAGGGCTCTGCTC	TGCCTTTTCCTCCTTGGCTGTTATC
NPPB	NM_008726.6	CTTTGGGCACAAGATAGACCGGATC	AGGCAGAGTCAGAAACTGGAGTCTC
SREBP1	NM_011480.4	TCTGAGGAGGAGGGCAGGTTCCA	GGAAGGCAGGGGGCAGATAGCA
FASN	NM_007988.3	GGCGGCACCTATGGCGAGG	CTCCAGCAGTGTGCGGTGGTC
SCD1	NM_009127.4	GGAAAGTGAGGCGAGCAACTGACTA	CAGGACGGATGTCTTCTTCCAGGTG
ACACA	NM_133360.2	GGAAGATGGCGTCCGCTCTGTG	GTGAGATGTGCTGGGTCATGTGGAC

Histological analysis

Formalin-fixed hearts were embedded in OCT compound (Optimum Cutting Temperature; Sakura Finetek Europe B.V., Alphen aan de Rijn, The Netherlands). Cryosections of 10 μm of the aortic root as well as the middle part of the heart were collected on Menzel Gläser SuperFrost® Plus slides (Thermo Scientific; USA). Sections were routinely stained for the presence of neutral lipids using Oil Red O and hematoxylin (Sigma-Aldrich, Zwijndrecht, The Nether-

lands). For identification of macrophages in sections containing atherosclerotic lesions, a primary monoclonal rat-anti-mouse Cd68 antibody (FA-11; ab53444; Abcam, Cambridge, UK) was used at a 1:1000 dilution in blocking buffer. A secondary AP-conjugated goat-anti-rat IgG (A8438, Sigma-Aldrich, Zwijndrecht, The Netherlands) was used at a dilution of 1:100 in blocking buffer. The ready-to use BCIP®/NBT liquid substrate system (sigma-Aldrich, Zwijndrecht, The Netherlands) was used for signal detection. Sections were stained using Masson's Trichrome (Sigma-Aldrich) to show the presence of collagen. Mean atherosclerotic lesion areas and macrophage areas (in μm^2) were quantified using pictures generated with a digital slide scanner (PANNORAMIC 250 Flash II, 3dHistech) and image J software. Quantification was performed blinded.

Flow Cytometry

Splenocytes were stained with antibodies directed against the cell markers CD4 and CD8 (T cells), CD19 (B cells), F4/80 (macrophages), Ly6G (neutrophils), Ly6C (monocyte/macrophages) and the T cell and macrophages polarization makers CD44, CD62L, MHCII, CD206 (eBioscience) in PBS containing 2% fetal bovine serum. Cell populations were also stained with efluor-780-viability (eBioscience) to identify viable cells. Flow cytometric analysis was performed on a Beckman Coulter Cytoflex S with FlowJo software.

Statistical analysis

Statistical analysis was performed using GraphPad Prism 8.0 (GraphPad Software Inc., San Diego, CA, USA). A Grubbs' test was used to test for outliers within groups. Two-tailed unpaired Student's t-test was used to calculate the significance of differences between single groups. A P-value below 0.05 was considered statistically significant for all tests. Data are presented in graphs as means ± SEM or individual points with respective group averages.

RESULTS

To test the hypothesis that the development of hypercholesterolemia and atherosclerosis can be restricted by inhibiting PRMT1-mediated hepatic lipogenesis, we treated LDL receptor knockout mice for 3 times per week with 10 mg/kg bodyweight TC-E or the solvent control DMSO by intraperitoneal injection, while feeding an atherogenic high cholesterol/high fat Western-type diet. Two and five weeks into the experiment, two TC-E-treated mice were unexpectedly found dead in their cage. We bled the remaining 11 control-treated and 9 TC-E-treated mice at the end of week 5 and found that blood glucose levels and body weights were not different between TC-E-treated mice and control mice (Fig. 1B & 1C). At week 6, another TC-E-treated mouse displayed signs of pathology, i.e. it had significantly lost weight and presented with a hard belly, which required early sacrifice. Given that the difference in survival rate almost reached significance (Fig. 1A; P=0.07 for survival curve comparison), we decided to terminate the study after 8 weeks of diet feeding and compound treatment to keep a sufficient sample size for statistical analysis. At this point, the two groups of mice still did not significantly differ in weight (Fig. 1B). During sacrifice we noted that the organs in the peritoneal cavity of TC-E-treated mice were sticking to each other, possibly due to in vivo compound insolubility and associated mucous membrane irritation [10]. Notably, Murata et al. found that mice with cardiomyocyte-specific PRMT1 depletion exhibit cardiac dysfunction and fibrotic heart disease and as a result die within 60 days after birth [11]. To investigate whether cardiac dysfunction contributed to the observed mortality in TC-E-treated mice, we performed histological staining on heart tissue sections. No obvious collagen accumulation was observed in TC-E-treated mice or in control mice (Fig. 1D). In addition, mRNA expression levels of cardiac dys-

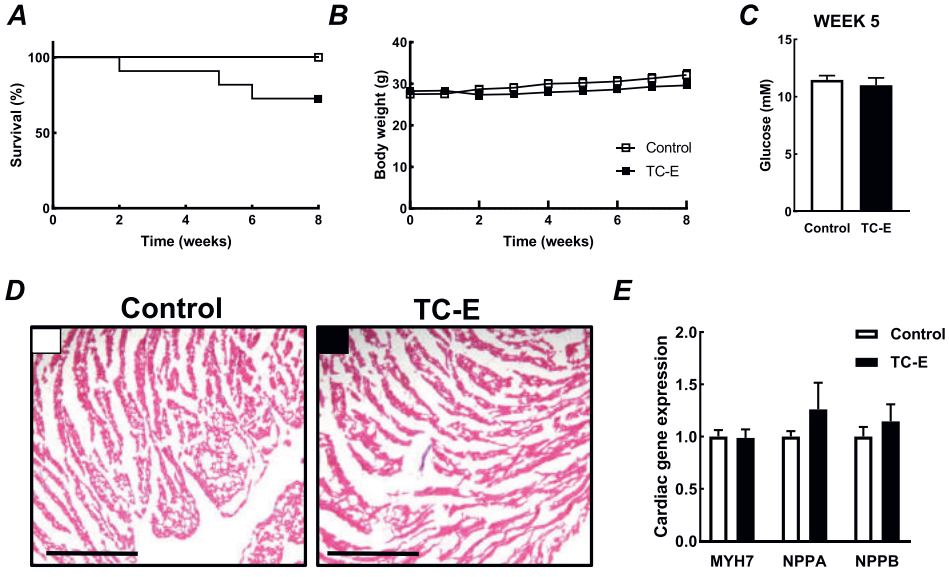

Figure 1: *TC-E 5003 treatment does not alter body weight, induce cardiac collagen disposition, or change basal gene expression levels in heart, while it reduces plasma cholesterol levels.*

*The survival rates (A) and body weights (B) of male LDL receptor knockout mice treated with DMSO solvent control (Control; white) or 10 mg/kg TC-E 5003 (TC-E; black) for 8 weeks under Western-type diet feeding conditions. (C) After 5 weeks of treatment, blood glucose were measured by tail bleeding. (D) Heart tissue cryosections were stained with Masson's Trichrome to visualize collagen. Scale bar = 200 µm. (E) Relative mRNA expression levels of MYH7, NPPA, and NPPB were measured in hearts. Data are expressed as means ± SEM. * P <0.05 (Two-tailed unpaired Student's t-test)*

function marker genes Myh7, NNPA, and NNPB in heart were not affected by TC-E treatment (Fig. 1E; t-test: P>0.05). As such, a negative effect of chronic TC-E treatment on cardiac function can likely be excluded.

To verify the potential ability of TC-E to prevent hyperlipidemia, we measured plasma lipid levels at sacrifice. TC-E-treated mice display a reduction in plasma cholesterol levels. More specifically, both plasma free cholesterol (-37%; P<0.05) and cholesteryl ester (-40%; P<0.01) levels were lower as compared to DMSO-treated control mice after 8 weeks of Western-type diet feeding (Fig. 2A). Measurement of specific lipoprotein fractions showed that mainly VLDL-

cholesterol and LDL-cholesterol levels were decreased by TC-E treatment. The amount of cholesterol transported by HDL particles remained at similar levels in both groups of mice (Fig. 2B). Given that VLDL particles contain high levels of triglycerides, TC-E treatment also significantly lowered the concentration of plasma triglycerides (-33%; t-test: P<0.05) (Fig.2A).

To understand the mechanism behind the TC-E treatment-mediated lowering of the hyperlipidemia extent, livers were isolated and analyzed biochemically. The mRNA expression levels of the lipogenic gene SREBP-1 (-31%; P<0.001)

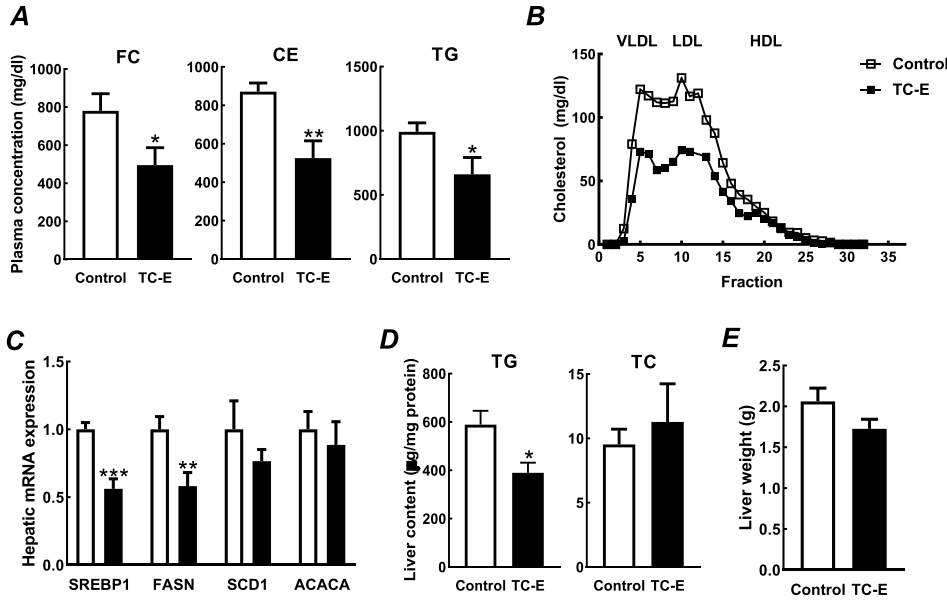

Figure 2: *TC-E 5003 treatment reduces the mRNA expression levels of genes involved in hepatic lipogenesis and lowers liver triglyceride accumulation and the hyperlipidemia level.*

*(A) Plasma triglyceride (TG), free cholesterol (FC) and cholesteryl ester (CE) levels in male LDL receptor knockout mice treated with DMSO solvent control (Control; white) or 10 mg/kg TC-E 5003 (TC-E; black) for 8 weeks under Western-type diet feeding conditions. (B) The distribution of very low-density lipoprotein (VLDL), low density lipoprotein (LDL) and high-density lipoprotein (HDL) fractions. (C) Relative mRNA expression levels of key genes involved in hepatic de novo lipogenesis. (D) Hepatic triglyceride and total cholesterol (TC) levels. (E) Liver weights. Data are expressed as means ± SEM. * P <0.05, ** P <0.01, *** P <0.001 (Two-tailed unpaired Student's t-test).*

and FASN (-42%; $P<0.01$) were both downregulated by TC-E treatment (Fig. 2C), suggesting a reduced hepatic lipogenesis rate after PRMT1 inhibition. The difference in liver SCD1 (-27%) and ACACA (-12%) relative mRNA expression levels between treatment and control did not reach statistical significance (Fig. 2C). In line with previous data of Bieghs et al., fatty livers of our Western-type diet-fed LDL receptor knockout control mice contained ~600 µg of triglycerides per mg protein [12]. As anticipated from the decrease in FASN expression, TC-E treatment also significantly lowered triglyceride accumulation in liver (-30%; $P<0.05$) without a parallel change in hepatic total cholesterol levels (Fig. 2D). However, no change was observed in total liver weight (Fig. 2E).

To confirm that the decreased fatty liver disease and lower serum cholesterol levels also translated into a reduced atherosclerosis development, sections of the aortic root were stained with Oil red O to identify neutral lipid stores. Both groups had developed stage III atherosclerotic lesions, characterized by areas of lipid-laden macrophage foam cells and the development of an early fibrous cap [13]. Quantification of the Oil red O lipid staining showed an average atherosclerotic lesion area of $20.5 \pm 7.6 \times 10^4$ µm^2 in control mice, while TC-E-treated mice contained average lesion areas of $15.3 \pm 4.8 \times 10^4$ µm^2 (Fig. 3A & 3B). The atherosclerotic lesions consisted mostly of CD68$^+$ macrophages and had a low amount of collagen as judged from the Masson's Trichrome staining (Fig. 3A). In further support of a decreased atherosclerotic lesion development, we observed that the total aortic macrophage area was around 2-fold lower in the TC-E-treated group as compared to the control group (Fig. 3C; $P<0.05$).

In addition to lipids, inflammation is a key mechanism involved in the pathogenesis of atherosclerosis [14]. For example, the splenic monocyte population is a driver of atherosclerotic macrophage/foam cell accumulation [15]. Since PRMT1 has been shown to also play a role in immunosuppression and immune cell proliferation [16] [17] [18], potential immune effects of TC-E treatment were investigated

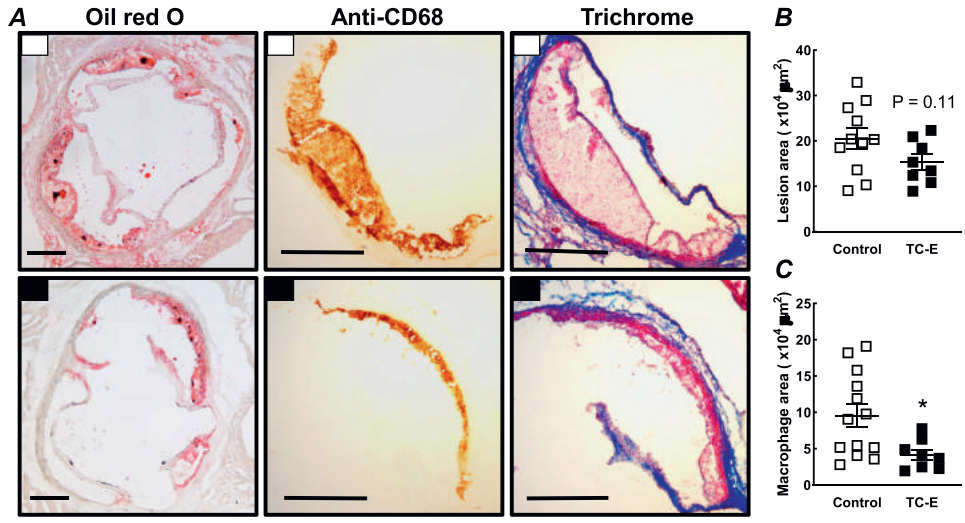

Figure 3: *TC-E 5003 treatment reduces atherosclerosis susceptibility.*

*(A) Representative pictures of aortic root cryosections from male LDL receptor knockout mice treated with DMSO solvent control (Control; white) or 10 mg/kg TC-E 5003 (TC-E; black) stained with Oil Red O (neutral lipids; red), an anti-CD68 antibody (macrophages; brown) or Masson's Trichrome (collagen; blue). Scale bar = 200 µm. Quantification of the total lesion areas (B) and lesional macrophage areas (C). Data are shown as individual points with the group average as horizontal lines. * P <0.05 (Two-tailed unpaired Student's t-test).*

in spleen. Ten to 15% of all splenocytes were identified as $Ly6C^{+}$ monocytes in both groups of mice using flow cytometry. Within this monocyte population, the $Ly6C^{high}/Ly6C^{low}$ cell ratio – a measure for the inflammatory activation [19] - was significantly decreased in TC-E-treated mice (Fig. 4A; t-test: $P<0.01$). No differences were found in the splenic relative $F4/80^{+}$ macrophage population nor in their mean expression values of the pro-inflammatory macrophage marker MHCII and the anti-inflammatory macrophage marker CD206 (Fig. 4B). $CD19^{+}$ B cell and $Ly6G^{+}$ neutrophil numbers in the spleen were also not changed by TC-E treatment (data not shown). Interestingly, we observed that TC-E treatment decreased the number of $CD4^{+}$ T lymphocytes by 10% ($P<0.01$; Fig. 4C).

However, the activation state of these T cells was increased. As shown in figure 4C, TC-E treatment was associated with a shift in the $CD4^+$ T cell population from naïve (N), resting cells (-16%; t-test: $P<0.001$) to more activated effector memory (EM) cells (+27%; t-test: $P<0.05$) in the context of an unchanged central memory fraction. The same change in T cell activation was observed for $CD8^+$ cells, since the relative amount of naïve $CD8^+$ T cells was also significantly decreased by TC-E treatment (-12%; t-test: $P<0.001$) and the fraction of $CD8^+$ effector memory T cells tended to increase (+57%; Fig. 4D).

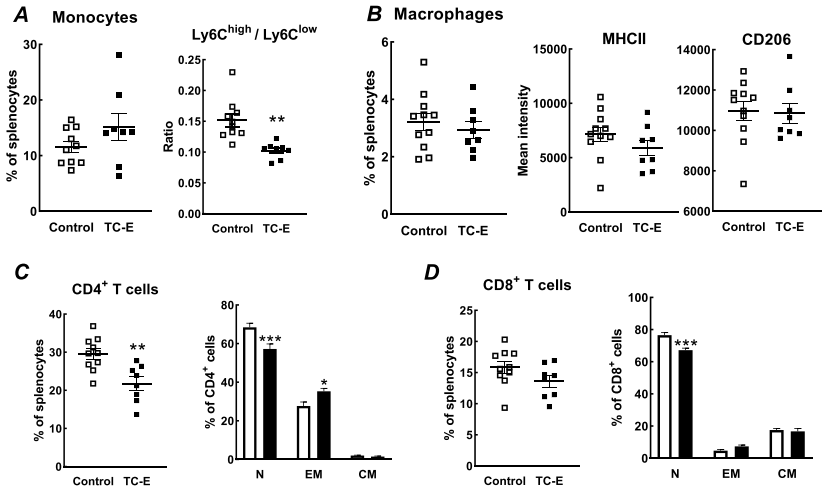

Figure 4: *TC-E 5003 treatment reduces monocyte activation and increases T cell activation.*

*(A) Relative numbers of monocytes (left) and the Ly6Chi / Ly6Clow ratio (right) within the Ly6C+ monocyte fraction in spleens of male LDL receptor knockout mice treated either with DMSO solvent control (Control; white) or 10 mg/kg TC-E 5003 (TC-E; black). (B) Relative numbers of splenic F4/80+ macrophages (left) and their mean intensities of the pro-inflammatory marker MHCII (middle) and the anti-inflammatory marker CD206 (right). Splenic relative numbers of (C) CD4+ T cells and (D) CD8+ T cells (left panels) and their distribution over the naïve (N), effector memory (EM), and central memory (CM) subtypes (right panels). Data are expressed as means ± SEM. * P <0.05, ** P <0.01, *** P <0.001 (Two-tailed unpaired Student's t-test).*

DISCUSSION

Here we have shown that the PRMT1 inhibitor TC-E 5003 effectively decreases hepatic triglyceride accumulation during high fat diet-induced fatty liver development and lowers the hyperlipidemia extent in LDL receptor knockout mice, resulting in a reduction in atherosclerotic lesion susceptibility.

We found that the TC-E treatment-induced reduction in liver triglycerides was paralleled by a decrease in the mRNA expression levels of SREBP1 and FASN, genes involved in hepatic fatty acid synthesis. These findings support our working hypothesis, originally derived from the findings of Park et al. [6], that PRMT1 is functionally involved in the transcriptional control of hepatic lipogenesis and thereby contributes to the development of NAFLD in mice. Notably, human patients with NAFLD exhibit 3-fold elevated hepatic de novo lipogenesis rates as compared to healthy individuals [3][17]. It can therefore be suggested that PRMT1 may possibly also be a therapeutic target to prevent the development of NAFLD in humans.

In line with the assumption that the hyperlipidemia in LDL receptor knockout mice is mainly attributed to highly activated hepatic de novo lipogenesis [12 21 22], the inhibition of PRMT1 effectively reduced the hyperlipidemia extent, i.e. VLDL/LDL levels, in our current experimental setup. However, since we did not measure food intake, it cannot be excluded that the reduction in plasma lipid levels was also, in part, due to an effect of TC-E treatment on general well-being and associated food consumption.

A previous study by Van der Laan et al. has shown that VLDL levels in plasma best predict the atherosclerotic plaque size in the aortic root of LDL receptor knockout mice [23]. Accordingly, the observed decrease in VLDL and LDL levels also translated into a reduction in the atherosclerotic lesion area in our TC-E-treated LDL receptor knockout mice. Hyperlipidemia in atherosclerotic LDL receptor knockout

mice has previously also been associated with an increase in pro-inflammatory monocyte numbers [24]. In line, we also observed a decrease in the inflammatory state of the monocytes within the spleen, as evident from a decrease in the $Ly6C^{hi}$/$Ly6C^{low}$ monocyte ratio. Given that $Ly6C^{hi}$ monocytes are precursors of infiltrated foam-macrophages accumulating in atherosclerotic plaques [15 19], it can be assumed that the decrease in atherosclerotic lesion size is not only related to the lower hyperlipidemia, but also secondary to the lower pro-inflammatory monocyte activation. Importantly, a recent in vitro study from Kim et al. showed that TC-E significantly reduces the NO production and the expression of inflammatory genes like inducible NO synthase, tumor necrosis factor-α, and interleukin-6 in lipopolysaccharide-stimulated RAW 264.7 monocytes/macrophages [17]. As such, the beneficial effect on the overall monocyte activation status can possibly also be attributed to inhibition of PRMT1's pro-inflammatory actions locally in monocytes.

In addition to the anti-inflammatory effect of TC-E treatment in monocytes, we observed that PRMT1 inhibition decreased CD4+ T cell numbers and shifted the polarization of CD4+ and CD8+ T cells from the naïve towards the more pro-inflammatory effector memory phenotype. In accordance with a potential role for PRMT1 in activating T cell proliferation, Sen et al. showed that pharmacological inhibition of PRMT1 by TC-E also decreases the amount of $CD4^+$ T cells in central nervous system in a mouse model of experimental autoimmune encephalomyelitis [18]. Kagoya et al. showed that PRMT1 interacts with forkheard box transcription factor 3 (FOXP3), which plays a crucial role in the differentiation of regulatory T cells that suppress $CD4^+$ and $CD8^+$ T cell activation [25]. The TC-E-mediated increase in T cell activation in our current study may thus perhaps be due to an impaired T regulatory cell function. Ait-Oufella et al. showed that regulatory T cells can suppress atherosclerosis development in LDL receptor knockout mice [26]. In addition, Olson et al. also showed that a shift in T cell polarization from the naïve to the memory phenotype is associated with high-

er cardiovascular disease risk in humans [27]. Combined, these findings suggest that the effect of TC-E treatment on T cell activation may have diminished the overall atheroprotective hypolipidemic effect of PRMT1 inhibition.

In conclusion, we have shown that PRMT1 inhibition is associated with reduced hepatic triglyceride accumulation, hyperlipidemia and monocyte activation in the context of increased T cell activation, resulting in an overall decrease in atherosclerosis susceptibility in Western-type diet-fed LDL receptor knockout

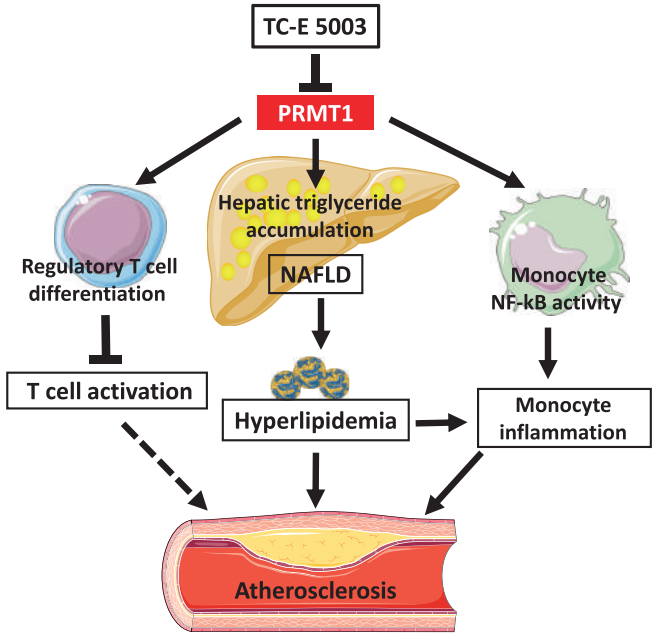

Figure 5: Proposed mechanism behind the anti-atherogenic effect of PRMT1 inhibitor TC-E 5003 treatment in Western-type diet-fed LDL receptor knockout mice.

Inhibition of PRMT1 activity by TC-E 5003 reduces hepatic triglyceride accumulation and thereby lowers the non-alcoholic fatty liver disease (NAFLD) susceptibility, which is accompanied by a reduction in pro-atherogenic hyperlipidemia and, as a result, a reduced pro-inflammatory monocyte activation. In addition, TC-E 5003 treatment directly inhibits pro-inflammatory monocyte development through inhibition of NF-KB activity. Furthermore, TC-E 5003 treatment inhibits regulatory T cell differentiation, resulting in a higher pro-atherogenic T cell activation that is apparently not sufficient to overrule the overall anti-atherogenic effect of TC-E 5003.

mice. Our study highlights (1) that PRMT1 influences both inflammatory and metabolic process in vivo (Fig. 5) and (2) that blocking specifically hepatocyte PRMT1 may be a valuable therapeutic approach to inhibit NAFLD, hyperlipidemia and atherosclerosis development.

ACKNOWLEDGMENTS

This study was supported by grants from the Netherlands Organization for Scientific Research (VICI 91813603) awarded to Miranda Van Eck. Miranda van Eck is head of the Cardiovascular and Metabolic Therapeutics group (https://www.universiteitleiden.nl/en/science/drug-research/biotherapeutics/cardiovascular-and-metabolic-therapeutics) and an Established Investigator of the Dutch Heart Foundation (2007T056). Yiheng Zhang is supported by the Chinese Scholarship Council (CSC).

AUTHOR CONTRIBUTIONS

Yiheng Zhang: Conceptualization, Investigation, Formal analysis, Data curation, Writing-Original draft preparation, Visualization. Timothy J.P. Sijsenaar: Investigation, Formal analysis, Data curation, Writing & Review manuscript, Visualization. Mireia N.A. Bernabé Klein: Investigation. Ezra J. van der Wel: Formal analysis, Data Curation. Miranda Van Eck: Supervision, Writing-Review & Editing, Funding Acquisition, Project administration, Menno Hoekstra: Conceptualization, Methodology, Supervision, Writing-Review & Editing, Project administration.

REFERENCES

1. Friedman, M. & Rosenman, R. H. Association of specific overt behavior pattern with blood and cardiovascular findings: blood cholesterol level, blood clotting time, incidence of arcus senilis, and clinical coronary artery disease. J. Am. Med. Assoc. 169, 1286–1296 (1959).
2. Kasper, P. et al. NAFLD and cardiovascular diseases: a clinical review. Clin. Res. Cardiol. 110, 921–937 (2021).
3. Donnelly, K. L. et al. Sources of fatty acids stored in liver and secreted via lipoproteins in patients with nonalcoholic fatty liver disease. J. Clin. Invest. 115, 1343–1351 (2005).
4. Angulo, P. GI epidemiology: nonalcoholic fatty liver disease. Aliment. Pharmacol. Ther. 25, 883–889 (2007).
5. Byrne, C. D. & Targher, G. NAFLD: a multisystem disease. J. Hepatol. 62, S47–S64 (2015).
6. Park, M.-J. et al. Thioredoxin-interacting protein mediates hepatic lipogenesis and inflammation via PRMT1 and PGC-1α regulation in vitro and in vivo. J. Hepatol. 61, 1151–1157 (2014).
7. Bissinger, E.-M. et al. Acyl derivatives of p-aminosulfonamides and dapsone as new inhibitors of the arginine methyltransferase hPRMT1. Bioorg. Med. Chem. 19, 3717–3731 (2011).
8. Shimano, H. & Sato, R. SREBP-regulated lipid metabolism: convergent physiology—divergent pathophysiology. Nat. Rev. Endocrinol. 13, 710–730 (2017).
9. Adams, M. L., Sullivan, D. M., Smith, R. L. & Richter, E. F. Evaluation of direct saponification method for determination of cholesterol in meats. J. Assoc. Off. Anal. Chem. 69, 844–846 (1986).
10. Https://www.caymanchem.com/msdss/17718m.pdf. No Title.
11. Murata, K. et al. PRMT1 deficiency in mouse juvenile heart induces dilated cardiomyopathy and reveals cryptic alternative splicing products. Iscience 8, 200–213 (2018).
12. Bieghs, V. et al. LDL receptor knock-out mice are a physiological model particularly vulnerable to study the onset of inflammation in non-alcoholic fatty liver disease. PLoS One 7, e30668 (2012).
13. Whitman, S. C. A practical approach to using mice in atherosclerosis research. Clin. Biochem. Rev. 25, 81 (2004).
14. Raggi, P. et al. Role of inflammation in the pathogenesis of atherosclerosis and therapeutic interventions. Atherosclerosis 276, 98–108 (2018).
15. Westerterp, M. et al. ATP-binding cassette transporters, atherosclerosis, and inflammation. Circ. Res. 114, 157–170 (2014).
16. Parry, R. V & Ward, S. G. Protein arginine methylation: a new handle on T lymphocytes? Trends Immunol. 31, 164–169 (2010).

17. Kim, E. et al. Protein arginine methyltransferase 1 (PRMT1) selective inhibitor, TC-E 5003, has anti-inflammatory properties in TLR4 signaling. Int. J. Mol. Sci. 21, 3058 (2020).
18. Sen, S. et al. PRMT1 plays a critical role in Th17 differentiation by regulating reciprocal recruitment of STAT3 and STAT5. J. Immunol. 201, 440–450 (2018).
19. Swirski, F. K. et al. Ly-6C hi monocytes dominate hypercholesterolemia-associated monocytosis and give rise to macrophages in atheromata. J. Clin. Invest. 117, 195–205 (2007).
20. Lambert, J. E., Ramos–Roman, M. A., Browning, J. D. & Parks, E. J. Increased de novo lipogenesis is a distinct characteristic of individuals with nonalcoholic fatty liver disease. Gastroenterology 146, 726–735 (2014).
21. Jahn, D., Kircher, S., Hermanns, H. M. & Geier, A. Animal models of NAFLD from a hepatologist's point of view. Biochim. Biophys. Acta (BBA)-Molecular Basis Dis. 1865, 943–953 (2019).
22. Karasawa, T. et al. Sterol Regulatory Element–Binding Protein-1 Determines Plasma Remnant Lipoproteins and Accelerates Atherosclerosis in Low-Density Lipoprotein Receptor–Deficient Mice. Arterioscler. Thromb. Vasc. Biol. 31, 1788–1795 (2011).
23. VanderLaan, P. A., Reardon, C. A., Thisted, R. A. & Getz, G. S. VLDL best predicts aortic root atherosclerosis in LDL receptor deficient mice*[S]. J. Lipid Res. 50, 376–385 (2009).
24. Hoekstra, M. et al. Hematopoietic upstream stimulating factor 1 deficiency is associated with increased atherosclerosis susceptibility in LDL receptor knockout mice. Sci. Rep. 11, 1–11 (2021).
25. Kagoya, Y. et al. Arginine methylation of FOXP3 is crucial for the suppressive function of regulatory T cells. J. Autoimmun. 97, 10–21 (2019).
26. Ait-Oufella, H. et al. Natural regulatory T cells control the development of atherosclerosis in mice. Nat. Med. 12, 178–180 (2006).
27. Olson, N. C. et al. Decreased naive and increased memory CD4+ T cells are associated with subclinical atherosclerosis: the multi-ethnic study of atherosclerosis. PLoS One 8, e71498 (2013).